Applied Catalysis B: Environmental 119–120 (2012) 329–339

Contents lists available at SciVerse ScienceDirect

Applied Catalysis B: Environmental

journal homepage: www.elsevier.com/locate/apcatb

Surface oxygen generated upon N_2O activation on iron containing ZSM-5 type zeolites with different elemental composition

Ayten Ates[a,*,1], Andreas Reitzmann[b,2], Gerrit Waters[c]

[a] Department of Chemical Engineering, Engineering Faculty, Cumhuriyet University, 58140 Sivas, Turkey
[b] Süd-Chemie AG Research and Development Catalytic Technologies, Waldheimer Str. 15, 83052 Bruckmühl, Germany
[c] Institute of Chemical Process Engineering, University Karlsruhe, Kaiserstraße 12, 76131 Karlsruhe, Germany

ARTICLE INFO

Article history:
Received 31 October 2011
Received in revised form 13 February 2012
Accepted 6 March 2012
Available online 14 March 2012

Keywords:
Nitrous oxide decomposition
Fe-ZSM-5
Multipulse method
Surface oxygen

ABSTRACT

Various ZSM-5 zeolites with iron contents ranging from of 0.86 to 4.98 and Si/Al ratios of 11.5–140 were prepared by solid-state ion exchange with $FeCl_2$. The catalysts were characterised by XRD, H_2-TPR and NH_3-TPD. The formation and stability of surface oxygen over these zeolites were investigated with a transient multipulse technique combined with subsequent temperature-programmed desorption (TPD). Higher iron contents enhance the formation of surface oxygen. However, when a critical iron content is reached, larger iron oxide clusters and particles are formed and these larger clusters do not contribute significantly to surface oxygen formation. Moreover, the amount of desorbed oxygen is more than that formed from N_2O due to the additional desorption of oxygen present in the lattice of such oxide clusters. TPD studies indicate the presence of different surface oxygen species depends on both the zeolite iron content and Si/Al ratio.

1. Introduction

The activation of nitrous oxide (N_2O) on various solid catalysts is accepted to be an important step in the partial oxidation of different hydrocarbons, such as hydroxylation of aromatics [1,2], oxidative dehydrogenation of propane [3,4] and epoxidation of propene [5,6]. Iron containing zeolites of the ZSM-5 type are efficient catalysts for all of these reactions. Extensive studies by Panov et al. [1,7,8] have shown that the surface oxygen formed in these zeolites, termed as α-oxygen, has remarkable features, including a very high reactivity for different substrates, and high selectivity, e.g. in the hydroxylation of benzene to phenol [1,7,8]. In addition, the data of Panov et al. suggest that the extent of α-oxygen formation is crucial for ZSM-5 zeolites to be active catalysts in the hydroxylation of aromatics as well as in the N_2O decomposition [7,8]. Recently Zhu et al. [9] reported results that supported Panov et al. [1,7,8]. In contrast, other authors have come to the conclusion that the presence of α-oxygen is not necessarily related to the activity of iron containing zeolites in the N_2O decomposition [10–16]. Thus, the role of ZSM-5 zeolite on surface oxygen for the activation of N_2O remains a point of vigorous debate.

Despite intense research, the zeolite characteristics that control the formation of surface oxygen are not known. Several factors contribute to the on-going uncertainty:

- Iron species can be introduced into the zeolites via different methods. Iron salts can be added into the synthesis mixture of zeolite. Subsequent high temperature calcination or steaming leads to the formation of extra-framework iron species [1,2,4,6,8,17–19]. Alternatively, iron species can be introduced post-synthetically through ion exchange. This technique has been carried out in the liquid phase using different iron salts as precursors [3,9–13,20–22] and in the gas phase using anhydrous $FeCl_3$ (chemical vapour deposition) [9,10,14–16,23–30]. Finally, although less often applied, solid-state exchange using combination of several iron salts has also been shown to be a suitable method [31–36].
- The location and identity of the iron species can be characterised by using different techniques. Temperature-programmed experiments, e.g. reduction with H_2 and CO as well as desorption of probe molecules or surface bound species [1,10,11,14,16,21–27,33,34], have commonly been applied. Spectroscopic methods have been used for directly identifying the iron species, e.g. Mössbauer [1,2,8,14,28,35], X-ray absorption [6,13–16,23,24,28–30], UV–vis [19,24,29–31] and EPR spectroscopy [1,2,16,19,27]. Different iron species, such as isolated

* Corresponding author. Current address: Department of Chemical Engineering, Massachusetts Institute of Technology, Cambridge, MA 02139, US.
E-mail addresses: ates@cumhuriyet.edu.tr, aates@mit.edu (A. Ates), andreas.reitzmann@sud-chemie.com (A. Reitzmann), gerrit.waters@basf.com (G. Waters).
[1] Tel.: +90 346 2191010/2248; fax: +90 346 2191179.
[2] Tel.: +49 80614903700; fax: +49 8061 4903704.

0926-3373/$ – see front matter © 2012 Elsevier B.V. All rights reserved.
doi:10.1016/j.apcatb.2012.03.004

cations, charged and uncharged dimers, and oligomers, as well as nano-sized and bulky iron oxide species, have been identified, but the quantification of certain species has been hardly possible, so far. Several studies demonstrate that some of these iron species always coexist in zeolites regardless of the preparation method, even if sometimes not assumed [2,14,24,28–30,33–35]. Results obtained by different research groups [9–13] clearly show that only a part of the iron is involved in the formation of surface oxygen, but the identification of the most important species remains a difficult task. The role of the characterisation technique in this debate was recently pointed out by Pirngruber et al. [29,37]. They emphasised that more than a single iron species must be responsible for forming surface oxygen only because of new interpretations of UV–vis and EXAFS data.

- Sophisticated methods have to be developed to measure the formation of surface oxygen and to determine the amount that can be deposited in the zeolite. For this purpose Panov and coworkers suggested a method containing batch experiments in a closed vacuum set-up [1,7,8,38], and this technique has also been used by other research groups [14,39]. In addition, transient response experiments have been performed in pulse and step mode [17,18,34,37,39], sometimes in the TAP reactor [40]. In order to distinguish different types of surface oxygen, isotope labelling and exchange studies were applied in different experimental techniques [1,10,29,38,41]. In Ref. [39], some of the methods have been compared. It was shown that both technique and conditions affect the determination of surface oxygen content.
- Results obtained by different research groups showed that the present of water in reaction mixtures decreases the amount of surface oxygen. El-Malki et al. reported that water introduced into reaction mixture decreased the rate of N_2O decomposition [16]. Zhu et al. reported that the water may convert active iron species into inactive oxide clusters, Fe_xO_y [42]. On the bases of step-response technique, Pringruber and Roy [10] and Kiwi-Minsker et al. [18] found the poisoning effect of water adsorbed on the active sites. Additionally, the theoretical study of Heyden et al. demonstrated that water may strongly affect the kinetics of N_2O decomposition and increase the apparent activation energy [43]. Bulushev et al. reported that O_2 formation in the gas phase is observed in the presence of water, which is about 25% of the amount of α-oxygen [44]. In addition to the foregoing results, Panov et al. reported a mechanistic investigation using IR spectroscopy, TPD and oxygen isotopes to study the interaction of water with both vacant α-sites and with adsorbed α-sites [45]. Water is adsorbed over the oxidised α-sites and Oα reacts with H_2O into O_2 and H_2. The amount of O_2 formed in this reaction is equal to half of the initial amount of α-oxygen. In contrast to the aforementioned findings, the discrepancy between surface oxygen amounts through the step- and the pulse-techniques and those measured by static-vacuum techniques in the iron containing zeolites was explained as an inhibition effect of water by Panov et al. [45].

In our previous investigations, we presented a multipulse method at ambient pressure combined with temperature-programmed desorption (TPD) to study the formation and stability of surface oxygen deposited in MFI zeolites during N_2O decomposition [34]. An advantage of this technique is capability for exclusively studying and quantifying the surface oxygen formation because low N_2O concentrations per pulse suppress side and consecutive reactions, such as NO and O_2-formation. Moreover, the method works at atmospheric pressure relevant for catalytic applications, and though not in vacuum [39]. In the present study, the multipulse technique has been applied to MFI zeolites with Si/Al ratios from 11.5 to 140 containing different iron amounts to show the impact of iron content and of zeolite structure's properties on the surface oxygen formation. Iron has been introduced through solid-state exchange since this method is the only one that allows for an exact adjustment of the desired iron amount [36]. In contrast to common way, in this investigation NH_4 forms of zeolites and $FeCl_2$ as sources have been used according to the method developed by Kögel et al. [32] in order to achieve a high Fe(II) fraction in the zeolite. Principally, the study is to contribute to the discussion how properties of iron containing ZSM-5 zeolites affect the formation and properties of surface bound oxygen species formed during N_2O activation.

2. Experimental

2.1. Preparation and characterisation of zeolites

Fe-ZSM-5 catalysts were prepared via solid-state ion exchange using NH_4-MFI and $FeCl_2{\cdot}4H_2O$ (Merk AG, Germany) according to the procedure given in Refs. [32,34]. Four commercially available MFI-zeolites provided as NH_4^+-form were used as parent zeolites. Their commercial code and Si/Al ratio were given by following:

- CBV2314 (Si/Al = 11.5), CBV5524G (Si/Al = 25), CBV 28014 (Si/Al = 140) supplied by Zeolyst Inc. (USA) termed as Z23, Z50 and Z280.
- SM27 (Si/Al = 11.5) supplied by Sued-Chemie AG (Germany) has also been used in our previous studies [34,39].

The zeolites were mixed intensely with the iron salt in a mortar at ambient conditions. Iron amount was adjusted to achieve a certain Fe/Al ratio in the zeolite. The mixture was heated up to 823 K within 3 h and maintained at this temperature in air for 6 h. Afterwards, the samples were cooled to room temperature, washed intensely with deionised water, dried at 393 K and calcined at 873 K in air for 1 h. Resulting samples are denoted as *X*Fe*Y* in which *X* and *Y* refer to the parent zeolite and the iron amount determined after ion exchange in % (w/w), respectively. The zeolites without iron were prepared through calcinations of the NH_4-form in air at 823 K for 6 h and termed as the parent samples Z23, Z50, Z280 and SM27.

Chemical composition of the samples was determined by inductively coupled plasma emission spectroscopy (ICP) (Table 1).

Structural characterisation of the zeolites was carried out with X-ray diffraction (XRD, Cu-Kα-radiation, PANalytical X'PERT PRO) (Table 1).

Micropore volume was determined from the argon sorption isotherm at 77 K (ASAP 2000, Micromeritics) applying the *t*-plot method (Table 1). Prior to the measurement, the samples were treated at 632 K for at least 12 h, as long as an absolute pressure of 10^{-1} Pa is reached.

Acid–base properties were determined through temperature programmed desorption of ammonia (NH_3-TPD) (TPD-NH_3, AutoChem 2910, Micromeritics, with detector: mass spectrometer, QMS422, Pfeiffer vacuum). The samples were saturated in a flow of 9.7% (v/v) NH_3/He at 323 K for 1 h, then purged with helium for 3 h and finally heated up to 973 K (ramp: 10 K min^{-1}), at which temperature they were maintained for 0.5 h.

Reducibility of iron species was measured with temperature-programmed reduction using H_2 (H_2-TPR) (TPR H_2, AutoChem 2910, Micromeritics, detector: mass spectrometer, QMS422, Pfeiffer vacuum). After 15 min at 323 K, samples were heated up to 1173 K in a flow of 5% (v/v) H_2/He (ramp: 10 K min^{-1}), at this temperature they were maintained for 0.5 h (flow rate: 25 cm^3 min^{-1} (STP)). Mass of samples was in the range of 0.5–1 g. In order to get reliable and comparable results, conditions were oriented on the Criterion developed by Monti and Baiker [46]. Several

Table 1
The characteristics of zeolites investigated.

Sample	Si/Al[a]	Fe[a] (w/w)	Fe/Al	Crystalline phases[b]	V_{MP}[c] ($cm^3\ g^{-1}$)	H_2/Fe[d] ($mol\ mol^{-1}$)
SM27	11.8	0.04	0.01	ZSM5	133	– (–)
SM27Fe4.98	14.2	4.98	0.85	ZSM-5 +Hematite	120	1.22 (1.14)
Z23	11.1	0.02	0.01	ZSM-5	144	– (–)
Z23Fe0.86	12.6	0.86	0.13	ZSM-5	138	1.30 (1.04)
Z23Fe2.09	12.8	2.09	0.32	ZSM-5	138	1.01 (–)
Z23Fe3.30	13.5	3.30	0.53	ZSM-5 + Hematite	132	0.92 (1.30)
Z23Fe3.88	15.0	3.88	0.70	ZSM-5 + Hematite	132	1.04 (–)
Z23Fe4.22	14.2	4.22	0.72	ZSM-5 +Hematite	130	0.86 (0.90)
Z50	27.3	0.02	0.01	ZSM-5	151	– (–)
Z50Fe0.93	30.5	0.93	0.34	ZSM-5	151	1.21 (0.96)
Z50Fe2.65	37.9	2.65	1.20	ZSM-5 + Hematite	145	1.0 (0.63)
Z280	118	0.03	0.04	ZSM-5	148	– (–)
Z280Fe1.13	113	1.13	1.44	ZSM-5	148	1.16 (–)
Z280Fe3.60	114	3.60	4.77	ZSM-5 +Hematite	137	1.51 (1.49)

[a] ICP.
[b] Phase composition obtained from XRD patterns.
[c] Micropore volume calculated from the sorption isotherms of argon at 77 K using *t*-plot method.
[d] H_2-TPR: total H_2 consumption per iron amount after treatment in helium, numbers in brackets after treatment in air.

physical mixtures of α-Fe_2O_3 and SM27 (provided by Sued-Chemie AG, Germany, Si/Al = 11.5, Na-form, designated as Na-MFI) and SiO_2 (Merck AG, Germany) were used as reference samples, as well as a sample prepared by incipient wetness impregnation of SiO_2 with $Fe(NO_3)_3$.

Prior to all temperature-programmed measurements (TPX), the zeolites were treated in a flow of helium or oxygen at 773 K for 2 h. Profiles obtained with both of the TPX methods were fitted and deconvoluted by using Gaussian functions, as explicitly shown in Ref. [34].

2.2. Determination of surface oxygen content and thermal stability

In the multipulse experiments, 0.1 g of catalyst was placed in a quartz reactor. Prior to the pulse sequence, all zeolites were pretreated by default in a helium flow of 50 $cm^3_{NTP}\ min^{-1}$ for 2 h at 773 K in order to remove adsorbed hydrocarbons for template containing zeolites and physisorbed water for all samples. Thereafter, 50 pulses of the mixture 1% (v/v) N_2O/1% (v/v) Ar/98% (v/v) He were injected to a flow of helium (10 $cm^3_{NTP}\ min^{-1}$) via a sample loop. Pulses each containing 0.31 μmol N_2O were given over the catalyst at 523 K. The area of each response peak in the multipulse sequence was integrated with the software MATLAB. The amount of surface oxygen deposited in the zeolites was calculated by summarising the areas of the N_2 pulses, and compared to the integrally converted N_2O. These values are termed as O/Cat(N_2) and ΔN_2O/Cat, respectively, if related to the zeolite mass, and O/Fe if related to the molar iron amount. After the pulse sequence, temperature was increased from 523 K to 1173 K with a ramp of 10 K min^{-1} in order to desorption of deposited oxygen species. The desorbed molecular oxygen is shown as atomic oxygen per catalyst mass, O/Cat(O_2). Further details of experimental procedure and analysis are described in Refs. [34,39].

Vacuum experiments were carried out with some samples in a batch system located in the Boreskov Institute of Catalysis (group of G.I. Panov) for comparison. Set up and experimental procedure are described in detail in Refs. [8,38,39], but a short summary is also given here. Before the experiment, the sample (1.0 g) was pretreated in vacuum at 823 K for 1.5 h followed by purging with O_2 (160 Pa) at 823 K for 1.5 h in order to remove adsorbed species. After decomposition of N_2O (267 Pa) on the zeolites at 493 K are

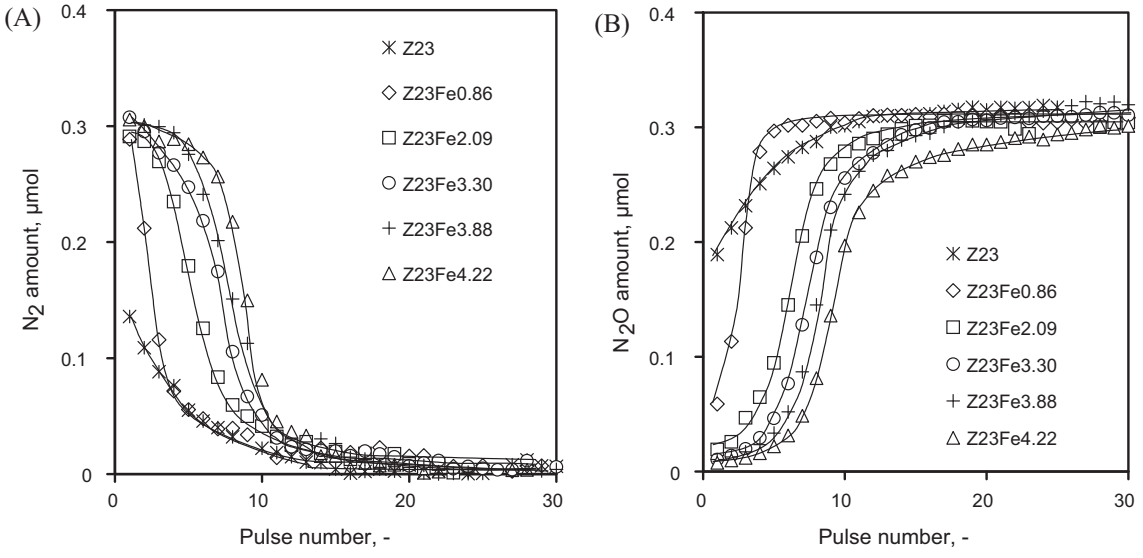

Fig. 1. The influence of iron amount in zeolite Z23 (Si/Al = 11.5) on the multipulse response behaviour: (A) N_2, (B) N_2O.

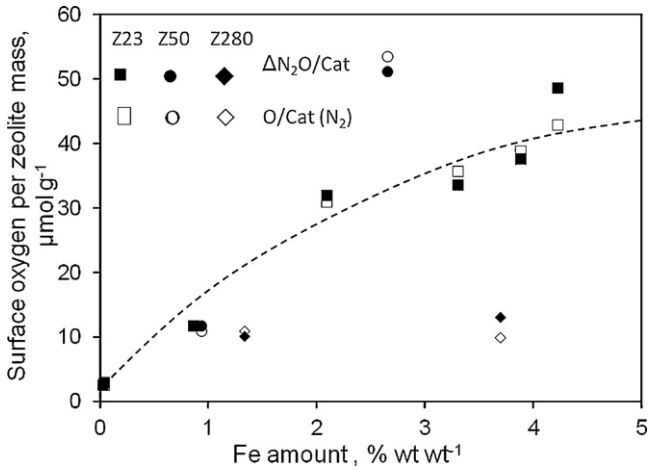

Fig. 2. Influence of iron amount in zeolites on surface oxygen formation: total N_2O conversion over pulse sequence (ΔN_2O/Cat, filled symbols), total N_2 formation over pulse sequence (O/Cat(N_2), open symbols.

performed for 20 min, the surface oxygen amount was measured using isotope exchange with $^{18}O_2$ (133 Pa) at 373 K.

3. Results and discussion

3.1. Formation and properties of surface oxygen for different zeolites

3.1.1. Amount of surface oxygen

Fig. 1 shows an example for the response on a sequence of N_2O pulses using the zeolite Z23 (Si/Al = 11.5) containing different iron amounts (see Table 1). Whilst N_2O pulses increase, N_2 pulses decrease with rising pulse number due to the formation of surface bound atomic oxygen. Since molecular oxygen was not formed during the pulse sequence on all samples, converted N_2O and formed N_2 can be directly used for quantifying the amount of surface oxygen. ΔN_2O/Cat and O/Cat(N_2) are shown in Table 2 and Fig. 2. They display that with increasing iron amount in Z23 the amount of surface bound oxygen increases. The most considerable rise is measured up to 2.09% (w/w) Fe in the zeolite (Z23Fe2.09) whilst higher iron loadings contribute less distinctive to the surface oxygen formation. As relating the surface oxygen amount to the molar iron content (Table 2: O/Fe), after at least 3.3% (w/w) Fe is introduced, a limit in O/Fe of approximately 0.06 is reached.

ΔN_2O/Cat was equal to O/Cat(ΔN_2) for zeolites containing up to 3.88% (w/w) Fe, but more N_2O was converted than N_2 formed in the sample with the highest iron content, Z23Fe4.22. Adsorption of molecular N_2O is responsible for the lack in the element balance which was also observed for SM27Fe4.98 (Table 2, Fig. 2) [34,39]. As determined in our previous work, the sorption of N_2O depends on certain iron species formed in the zeolites with high iron content.

Whilst quantitative results obtained for SM27Fe4.98 follow the trend shown for the Z23 samples (Fig. 2), the H-form of SM27 displayed a lower O/Fe value than Z23. The difference may result from the fact that SM27 was prepared through a template-free synthesis in contrast to Z23 crystallised with organic template. Burning off the organic template is known to cause structural changes in the zeolite framework, which can directly alter the iron species as described by Bordiga et al. [47] or the local environment of iron due to the formation of extraframework aluminium as described by Marturano et al. [15]. Both factors may affect the ability of zeolite to form surface oxygen in the N_2O activation.

Pulsing N_2O over zeolites with higher Si/Al ratios shows that introducing more iron promotes surface oxygen formation only in Z50, but not in Z280 (Table 2). In the case of Z50, higher iron contents even lead to an increase of the O/Fe value. Thus, results obtained with iron containing Z50 and Z280 do not follow the trend line in Fig. 2 marked by iron containing Z23 zeolites. High iron amounts introduced into Z50 and Z280 provide relatively more sites and less sites for surface oxygen formation, respectively, than that of Z23 with comparable iron contents. Therefore, the formation of active iron species necessitates the presence of an optimal Si/Al ratio. This ratio is not important for lower iron loaded catalysts because Fe^{3+} cations for an Fe/Al ratio of 0.56 are exchanged with the protons of the Bronsted acid sites on a one-to-one basis and formed dispersed cations such as $Fe(OH)^{2+}$, $Fe(OH)^{+}$ and FeO^{+} [33]. Since Fe/Al ratio of the catalysts with low iron loading is less than 0.56 as seen in Table 1, the conclusion has been done for higher iron loadings. This will be further discussed in the following sections.

3.1.2. Thermal desorption of surface oxygen for different zeolites

The thermal stability of surface oxygen was studied by TPD experiments after the N_2O multipulse sequence (Fig. 3). According to Kiwi-Minsker et al. [18] and Yoshida et al. [48], O_2 desorption profiles and corresponding O_2 amounts characterise the role and reactivity of surface oxygen in N_2O decomposition and reduction as well as in partial oxidation.

In the case of Z23, significant O_2 desorption was only detected for samples containing at least 2.09% (w/w) Fe (Fig. 3(A)). The higher the iron content is, the lower is the temperature when O_2 desorption starts, e.g. 900 K for Z23Fe2.09 and 700 K for Z23Fe4.22. The range of desorption temperature is in line with the observations made for SM27Fe4.98 [34,39] and MFI zeolites with different iron contents (Si/Al = 11.9, Fe/Al = 0.05–0.4) investigated by Kunimori and co-workers [21,48,49]. As in the case of the Z23 samples, they also found that O_2 desorbs in two strongly overlapped peaks over a broad temperature range. In the case of Z50Fe2.65, the two steps of O_2 desorption are more clearly visible showing maxima at 750 K and 1150 K. In contrast, Z280Fe3.60 exhibited only one O_2 desorption peak at 1150 K (Fig. 3(B)) indicating a very strong binding of surface oxygen.

Regarding all zeolites, O_2 desorption indicated the presence of different surface oxygen types, corroborating our previous findings for SM27Fe4.98 and results of other groups [10,13,18,34,39–41]. Moreover, data in Table 2 reveal that the amount of oxygen desorbed (O/Cat(O_2)) from Z23Fe2.09 and Z23Fe3.30 is equivalent to almost the oxygen amount formed (O/Cat (N_2) upon N_2O decomposition. Regardless the Si/Al ratios, O_2 desorption cannot be quantified for zeolites with iron contents lower than 1% (w/w). Zeolites with high iron contents, Z23Fe3.88, Z23Fe4.22 and Z50Fe2.65, release significantly more oxygen as formed during the N_2O pulses. Both of these phenomena were already reported for the two SM27 samples containing natural impurities and very high amounts of iron [34] (Table 2). Now, it becomes however clear that an "invisible" as well as an excessive O_2 desorption should be dictated by certain iron species formed in zeolites with very low and very high iron contents, respectively. Moreover, the density of negative charges in the zeolite plays not only a role for the sites of surface oxygen formation, but also for the properties of surface oxygen.

3.1.3. Influence of pre-treatment

Pre-treatment of iron containing zeolites is assumed to have a crucial impact on formation and properties of surface oxygen. According to the literature, the pre-treatment in helium at 773 K forms iron(II) species through autoreduction [10,17,18,20,24,29,33,41,48]. In order to investigate their role on the N_2O activation, several Z23 samples were treated additionally in air at 823 K for 2 h prior to the N_2O pulse sequence (Table 3, Fig. 4).

Table 2
Quantitative results of multipulse sequence and TPD for all zeolites investigated.

Sample	O/Cat (N_2)[a] (μmol g^{-1})	O/Fe[b] (mol mol^{-1})	ΔN_2O/Cat[c] (μmol g^{-1})	O/Cat(O_2)[d] (μmol g^{-1})
SM27	3	0.412	3	n.d.
SM27Fe4.98	41	0.046	50	56
Z23	3	0.726	3	n.d.
Z23Fe0.86	12	0.077	12	n.d.
Z23Fe2.09	31	0.083	32	28
Z23Fe3.30	36	0.061	34	39
Z23Fe3.88	39	0.056	38	58
Z23Fe4.22	43	0.057	49	58
Z50	–	–	–	–
Z50Fe0.93	11	0.066	12	n.d.
Z50Fe2.65	54	0.113	51	60
Z280	–	–	–	–
Z280Fe1.13	10	0.054	10	n.d.
Z280Fe3.60	10	0.016	13	10

[a] Formed N_2 during pulse sequence = surface oxygen.
[b] O/Fe: surface oxygen amount per Fe amount.
[c] Converted N_2O amount per catalyst amount.
[d] O_2 desorbed during TPD in helium up to 1173 K, given as atomic oxygen.

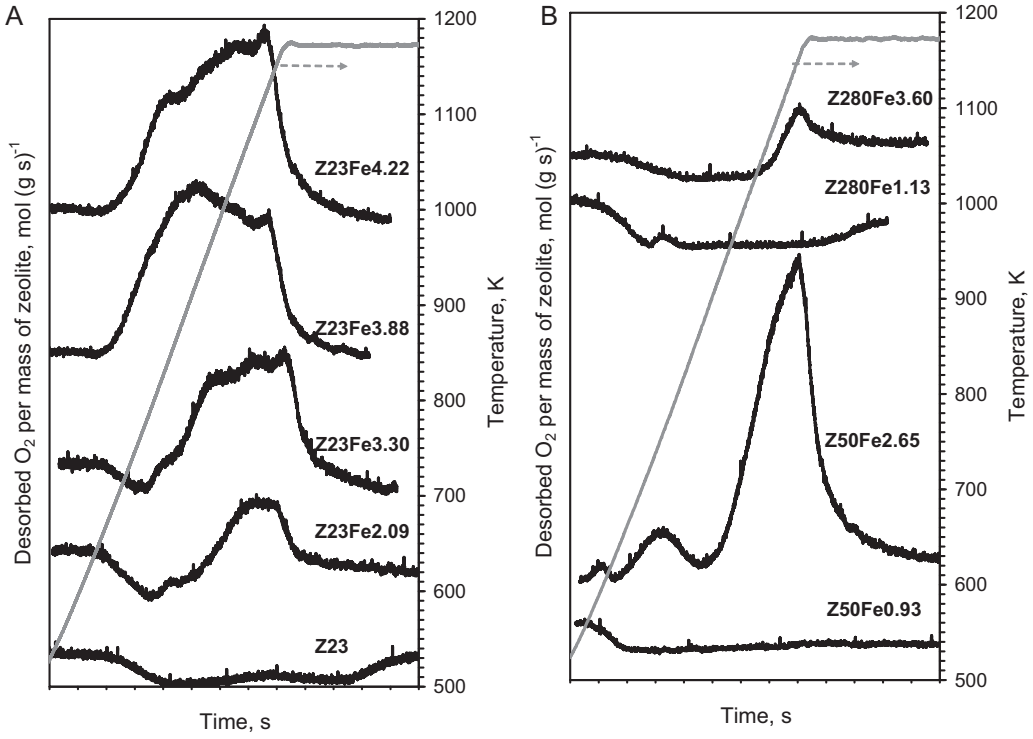

Fig. 3. (A) TPD of O_2 after the N_2O pulse sequence for Z23. (B) TPD of O_2 after the N_2O pulse sequence for Z50 and Z280.

Table 3
Influence of zeolites' pre-treatment on surface oxygen formation and oxygen desorption.

Sample	Treatment	O/Cat (N_2)[a] (μmol g^{-1})	O/Fe[b] (mol mol^{-1})	O/Cat(O_2)[c] (μmol g^{-1})
Z23	823 K, He, 2 h	3	0.726	n.d.
	823 K, Air, 2 h	3	0.726	n.d.
Z23Fe3.30	823 K, He, 2 h	36	0.061	39
	823 K, Air, 2 h	22	0.038	22
Z23Fe4.22	823 K, He, 2 h	43	0.057	58
	823 K, Air, 2 h	26	0.034	51

[a] Formed N_2 during pulse sequence = surface oxygen.
[b] O/Fe: surface oxygen amount per Fe amount.
[c] O_2 desorbed during TPD in helium up to 1173 K, given as atomic oxygen.

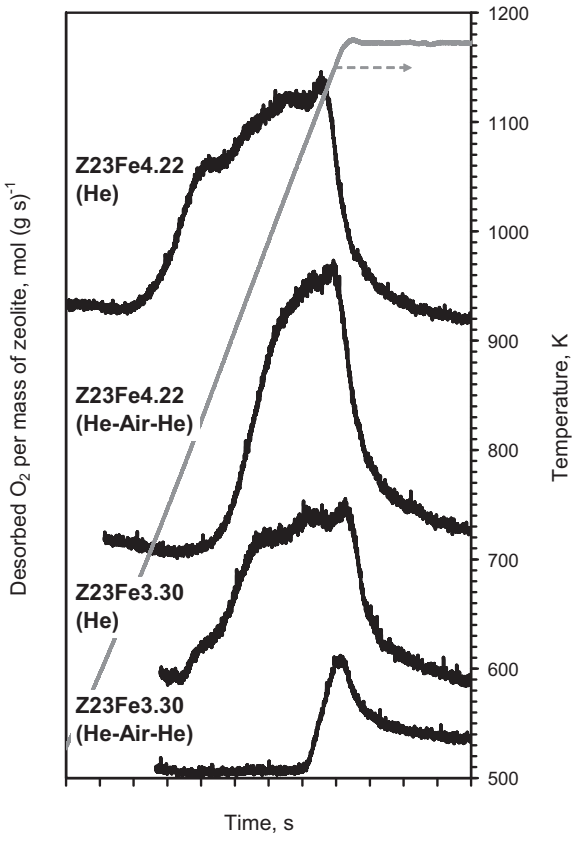

Fig. 4. Influence of the zeolite's pretreatment on the TPD of O_2 after the pulse sequence: He: 773 K, helium for 2 h; He–air–He: 773 K, helium for 2 h → 823 K, air for 2 h → 773 K, helium for 2 h.

In the case of zeolites containing only "natural" iron impurities, the pre-treatment atmosphere did not affect the surface oxygen formation and O_2 desorption up to 1173 K (Table 3). In contrast, approximately 40% less surface oxygen was formed after pre-treating samples with higher iron contents in air. In the subsequent temperature-programmed experiment, both of the samples also released less O_2. The comparison in Fig. 4 shows that after air pre-treatment, O_2 desorption from both of the zeolites was shifted to higher temperatures.

It has to be mentioned that the samples were also purged in helium for 2 h after calcination in air at the same temperature. This means that the status of the fresh samples cannot be re-obtained by a thermal treatment in inert gas. A similar behaviour was previously shown for the SM27 samples after pre-treatment in N_2O [34]. This may be due to the irreversible oxidation of Fe(II) species formed through autoreduction in He by N_2O. The present results extend this conclusion so that this process can also be carried out with molecular oxygen which not only inhibits the surface oxygen formation, but also alters the nature of surface oxygen species. However, these conclusions are obviously only valid for iron containing ZSM-5 prepared by means of solid-state exchange procedure. Zeolites with very low, "natural" iron impurities were found to be resistant to an O_2 treatment, corroborating the original idea of α-sites' nature developed by Panov et al. They stated that iron sites which can activate O_2 do not belong to α-sites [1,7].

3.1.4. Surface oxygen determined in the vacuum set-up: α-oxygen

In order to compare amount and nature of surface oxygen species determined with the features of α-oxygen, it was possible to perform experiments with some of the zeolites in the vacuum set-up. The results are shown in Fig. 5.

N_2 amount formed and N_2O amount converted during the N_2O decomposition at 493 K correspond well to the amount of $^{18}O_2$ isotopes exchanged with the α-oxygen loaded zeolites at 373 K (not shown). The comparison in Fig. 5(A) shows that the amount of surface oxygen determined by the multipulse method is slightly higher, but still in the range of α-oxygen in the case of samples with high iron contents corresponding to the results obtained for SM27Fe4.98 [39]. In contrast, samples with low iron contents, Z23Fe0.86 and Z50Fe0.93, form less α-oxygen than surface oxygen formed during the N_2O pulses. Hence, N_2O decomposition under ambient pressure forms additional surface oxygen species besides of only α-oxygen following the classical definition. Fig. 5(B) shows that the amount of oxygen desorbed was similar for Z23Fe3.30 regardless the method applied for N_2O activation. In the case of samples with lower and higher iron contents, the amount of desorbed oxygen was found to depend on method and respective conditions: in the vacuum set-up more and less oxygen desorbed from zeolites with low and high iron contents, respectively. The discrepancy for Z23Fe4.22 corresponds to results obtained with SM27Fe4.98 [39]. Furthermore, it has to be mentioned that the oxygen desorbed up to 823 K covers the amount of formed α-oxygen, but only a minor part desorbed up to this temperature after the N_2O multipulse sequence (Figs. 3 and 4). Finally, in contrast to results obtained with the multipulse method, it has no influence on formation and thermal stability of surface oxygen if zeolites were pretreated in O_2 or He in the vacuum set-up (not shown).

The observed discrepancies between N_2O activation studied in multipulse experiments under atmospheric pressure and in the closed vacuum set-up of Panov and co-workers under strongly reduced pressure lead obviously to different results (Fig. 5). Therefore, conclusions about formation and nature of surface oxygen depend on the method as previously shown for SM27Fe4.98 [39]. Now, it becomes clear that different results are not only obtained for zeolites with high iron contents. At first, more surface oxygen is formed at atmospheric pressure than that in the vacuum set-up. This may be due to an enhanced desorption and no accumulation of surface species at strongly reduced absolute pressure. However, particularly, the release of molecular oxygen from zeolites with low and very high iron contents during TPD is strongly affected by the apparatus and the applied conditions. Although this is not totally clear at the moment, it is firstly believed that the status of zeolite is different before N_2O activation: At low system pressures, zeolites and involved iron species are more severely dehydroxylated during the pre-treatment, which forms additional sites for α-oxygen stabilisation [1,7,8,10,14,17,38,39]. Note that a pre-treatment of the zeolites with O_2, as performed by default, does not affect the activation of N_2O which was obviously not the case at atmospheric pressure before the N_2O pulse sequence (Fig. 4, Table 3). Moreover, since the vacuum set-up is closed, zeolites are maintained in the dehydroxylated status obtained during pre-treatment. Moreover, very low amounts of gaseous impurities in the closed vacuum set-up, as traces of water as stated above, minimise any inhibiting effect of them during all experiments for determination of α-oxygen amount and particularly α-oxygen desorption. Nevertheless, in contrast to static-vacuum setup, the presented investigations concerning N_2O activation and surface oxygen formation under atmospheric pressures conditions give information useful for industrial applications performed under atmospheric pressure.

3.2. Characteristics of the zeolites

3.2.1. Elemental analysis

ICP analysis revealed that Si/Al ratios of parent zeolites are in the range of the values provided by the manufacturers. After the solid-state exchange with $FeCl_2$, Si/Al ratio increased for all

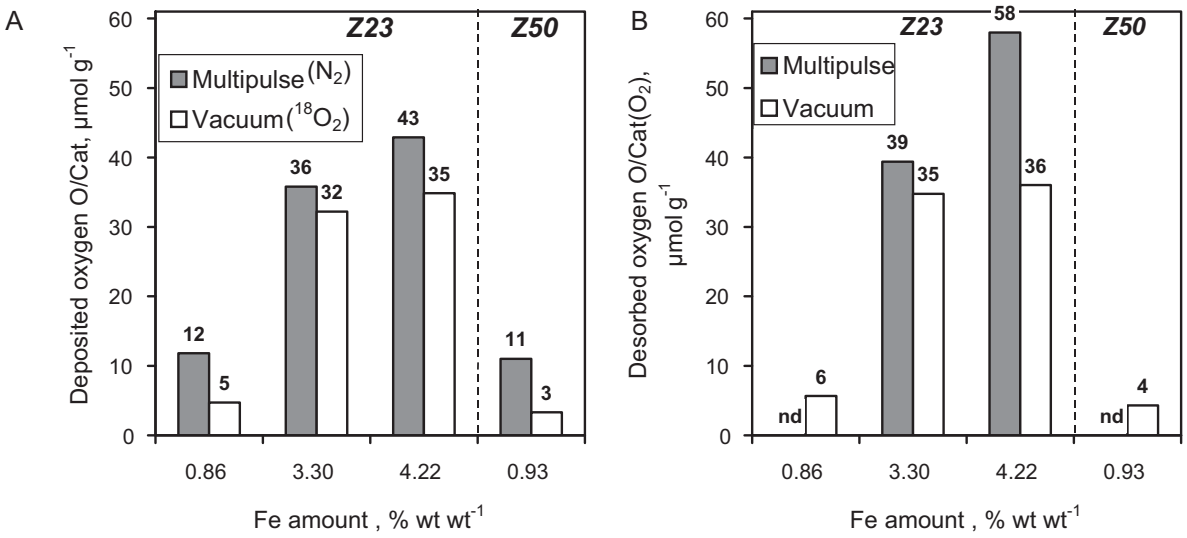

Fig. 5. Comparison of results obtained in multipulse experiments (filled bars) and in vacuum (open bars): (A) deposited surface oxygen, (B) desorbed oxygen up to 1173 K after multipulse sequence and up to 823 K after $^{18}O_2$ exchange in the vacuum set-up.

zeolites, except for Z280. The more iron salt is provided in the $FeCl_2/NH_4$-ZSM-5, the higher is the Si/Al ratio in the final zeolite. This unexpected observation should result from an aluminium extraction out of the zeolite in one step of the preparation procedure. The responsible step is not identified at the moment. Possibilities are that (i) dealumination of the zeolite framework occurred during calcination of the $FeCl_2/NH_4$-ZSM-5 mixtures in which HCl is formed, and/or (ii) extraframework Al species are already present in parent samples which can be extracted in the subsequent washing step. HCl formed in the washing solution is known to act as dealumination agent [50]. The most important conclusion on the preparation procedure is that it is not possible to get exactly the Fe/Al ratio desired in the preparation, as generally reported [36].

3.2.2. XRD and surface characteristics of samples

Iron contents of more than 2.5–3% Fe (w/w) in all samples lead to the formation of crystalline oxide species detectable as hematite in XRD (Table 1, 5th column). They have been identified via very low reflectances at 2θ angels of 33.2 and 35.7 (diffraction patterns not shown) [32,35,51,52]. In order to be detectable, crystalline oxides should be bigger than 3–4 nm [22,52]. Therefore, they should be located at the outer surface of zeolite crystals [22,32,52]. However, as soon as they can be observed in XRD, the micropore volume of the zeolite is significantly reduced (Table 1, 5th column). This indicates that larger oligomeric iron oxide clusters are also formed inside the channels when exceeding iron loadings of 2.5–3% (w/w). Interestingly, neither XRD nor the determined micropore volume indicated the formation of bulky iron oxide clusters in the case of Z280Fe1.13 exhibiting a very low number of negative charges for stabilising cations. Thus, it seems to be possible that well dispersed iron-oxo-clusters can also be generated in zeolites containing a low number of Brønsted acid sites when applying this kind of solid-state method.

3.2.3. NH_3-TPD

Fig. 6 shows the influence of iron species on the TPD profiles of NH_3. The high temperature (HT) peak of the profiles is related to the number of Brønsted acid sites [53]. The presence of iron cations should decrease the area of this peak as observed also in Refs. [33,34,52]. The low temperature (LT) peak cannot unambiguously be related to certain acid sites. Physisorbed NH_3, Lewis and weak Brønsted acid sites represented by cations or other extraframework species are suggested to be responsible for this peak [27,33,53].

All iron containing Z23 samples showed a reduced high temperature peak as compared to the protonic form (Fig. 6(A)). After deconvoluting the profiles with two Gaussian functions, however, it can be estimated that the introduction of 0.86% (w/w) Fe already reduced the area of the HT peak by approximately 50%. Regarding the Fe/Al ratio of 0.13 for this sample (Table 1), this would mean that more than one negative charge was compensated through the introduced iron species. Higher iron amounts lead to only a slightly further reduction of the HT peak area. Considering the Fe/Al ratios for zeolites containing at least 3.30% (w/w) Fe (Table 1), the reduction of the HT peak area corresponds approximately to a compensation of negative charges in the zeolite on a 1:1 basis. However, these samples contain crystalline Fe_2O_3 visible in XRD and probably also larger oxide clusters reducing the micropore volume (Table 1). On the bases of these results, it can be assumed that the iron species compensate more than one negative charge in Z23.

In contrast to the Z23 samples, the solid-state exchange of iron has a weaker effect on NH_3-TPD profiles of iron containing Z50 samples (Fig. 6(B)). The HT peak area decreases by 5–10% as compared to the parent Z50, but at the same time the LT peak increases by the same extent. Thus, the total amount of NH_3 desorbed from the Z50 samples is not significantly affected by the presence of iron species. This was unexpected when assuming a compensation of negative charges by iron cations as in the case of Z23. However, this effect was even more pronounced for the Z280 samples. The iron introduction into Z280 leads to a slight increase of the total NH_3 amount desorbed (Fig. 6(C)) because the HT peak area was not altered, but the LT peak area increased by 5–10%.

Although NH_3-TPD is known to be not an exact technique to quantify the influence of ion exchange on the number of Brønsted sites in zeolites, Lobree et al. have shown that results of NH_3-TPD correspond well to the number of bridged hydroxyl groups determined by FTIR for a ZSM5 zeolite (Si/Al = 27) exchanged with different amounts of $FeCl_3$. Both of the characterisation methods have shown that iron cations can replace up to approximately 60% of Brønsted acid protons [33]. A likely explanation for our discrepant finding was given by Sugawara et al. using an aqueous ion exchange method [21] and by El-Malki et al. using either the CVD [27] or the solid-state exchange technique [16]. Both of these groups observed that bands for bridging hydroxyl groups in

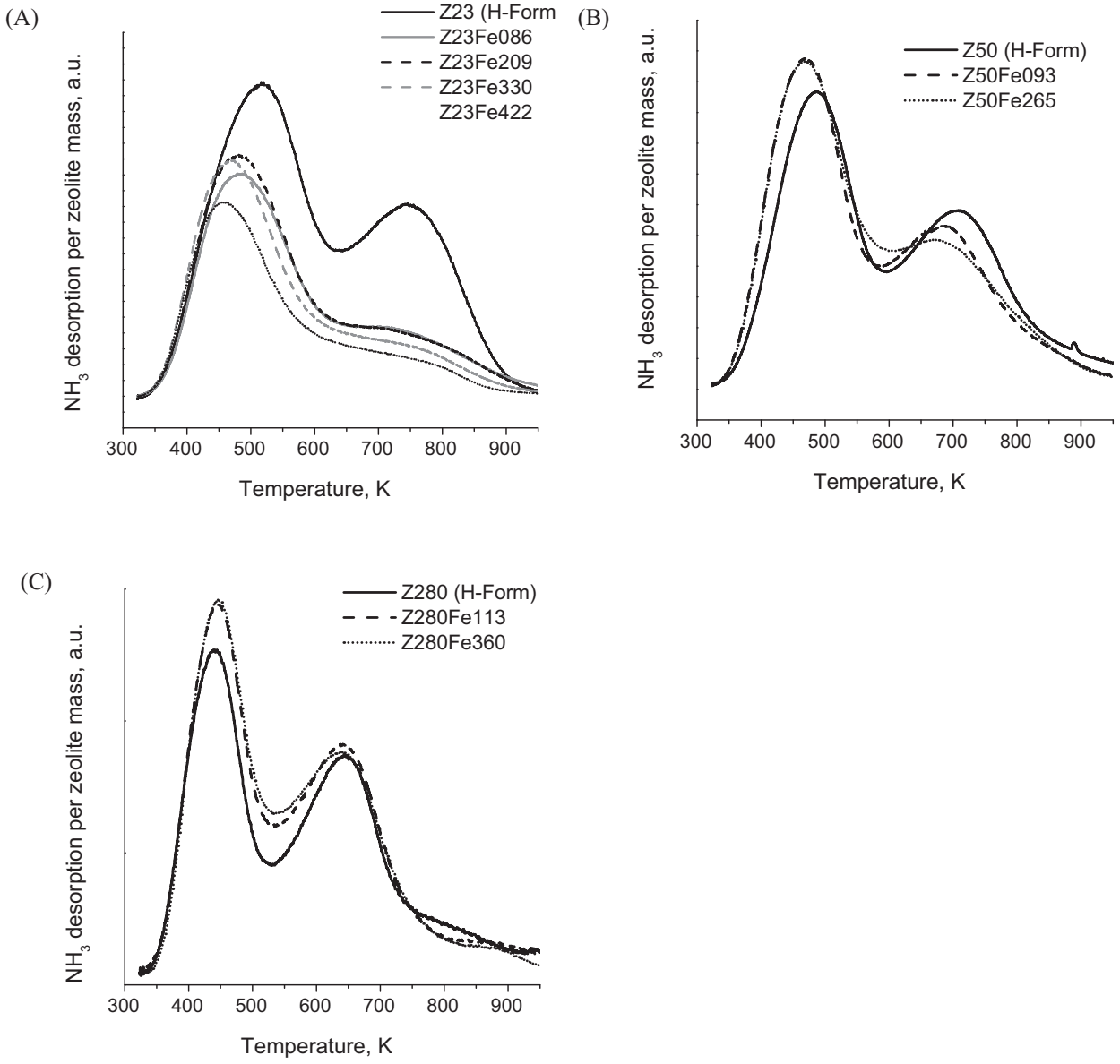

Fig. 6. Influence of iron introduction on the acid base properties of the zeolites (NH_3-TPD): (A) Z23, (B) Z50 and (C) Z280 with different iron contents.

FTIR have significantly been reduced or even disappeared after ion exchange. Both of them proposed that binuclear oxygen-bridged iron cations are the dominant species in ZSM-5 zeolites with high iron content. These clusters act as sites for strong NH_3 sorption and appear therefore as Brønsted and strong Lewis sites in NH_3-TPD [21,27]. In addition, an introduction of iron into lattice defects forming Brønsted sites is also possible, particularly for zeolites with lower Si/Al ratio, as shown by El-Malki et al. using a variety of characterisation techniques [27]. This means for the present study that the compensation of Brønsted acid protons by iron cations can only be detected in NH_3-TPD when isolated cations are present, as for Z23 with low iron contents. In the case of higher iron contents and lower Si/Al ratio, the formation of bi- and oligonuclear iron-oxo/hydroxo-species generates acid sites with similar strength as Brønsted acid protons, so that the charge compensation cannot be observed anymore by means of NH_3-TPD. The increase of the LT peak in NH_3-TPD of iron containing Z50 and Z280 zeolites should be attributed to the formation of Lewis acid sites, such as iron cations and small oxide clusters, corroborating El Malki et al.'s results of FTIR investigations with zeolites after pyridine adsorption [27].

3.2.4. H_2-TPR

Temperature-programmed reduction experiments were carried out to get further insights into iron species and their redox properties. The obtained profiles are shown in Fig. 7. The nature of the iron species present in the zeolites is commonly discussed on basis of the position of the H_2 consumption peaks and the consumed H_2 per mole of Fe (Table 1). Several research groups suggest that the reduction of Fe(III) to Fe(II) in isolated or binuclear oxo- and hydroxo-cations and -small oxide clusters proceeds at temperatures lower than 650–700 K and the area of the corresponding peak is characterised by a H_2/Fe ratio of 0.5 [22–24,26,33–35,47,51,52,54]. A further reduction of Fe(II) cations to Fe(0) proceeds at temperatures higher than 1000–1100 K, accompanied by a partial collapse of the zeolite structure [22,26,51,52]. Peaks in the temperature range 700–1000 K are mostly attributed to the reduction of Fe(II) in oxides to Fe(0) [22,24,51,52,54]. These peaks are often used to distinguish oxides from cations because reduction of Fe(III) to Fe(II) in both species proceeds in the same temperature range [24,35,54]. The ratio between H_2 consumption at temperatures higher and lower than

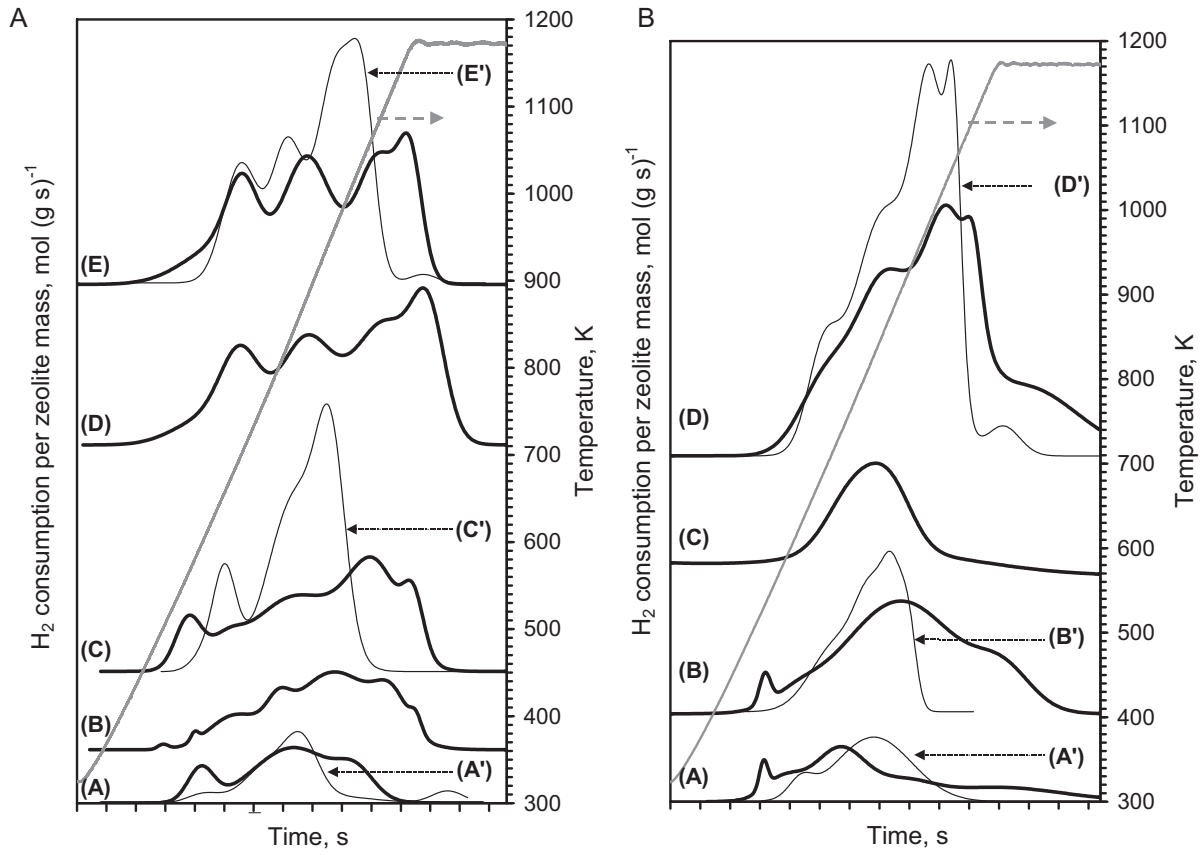

Fig. 7. (A) TPR with H_2 for Z23 zeolites with different iron contents: (A)/(A′) Z23Fe0.86, (B) Z23Fe2.09, (C)/(C′) Z23Fe3.30, (D) Z23Fe3.88, (E)/(E′) Z23Fe4.22; (A)–(E): pre-treated in helium at 773 K for 2 h (thick lines), (A′), (C′), (E′) pretreated in 5% O_2/Ar for 2 h (thin lines). (B) TPR with H_2 for Z50 and Z280 zeolites with different iron contents: (A) Z50Fe0.93, (B) Z50Fe2.65, (C) Z280Fe1.13, (D) Z280Fe2.60; (A)–(D): pre-treated in helium at 773 K for 2 h (thick lines), (A′), (B′), (D′) pretreated in 5% O_2/Ar for 2 h (thin lines).

≈700 K is used for estimations concerning how much iron oxide is present [35,51,54].

The reduction of all Z23 samples started at approximately 500 K (Fig. 7(A)). Z23Fe0.86 shows a first peak with a maximum at 600 K and two overlapping peaks with maxima at 820 and 970 K. In the sample containing 2.09% (w/w) iron, an additional peak with a maximum at about 680–700 K appears, which significantly increases for the samples with higher iron loadings. The first peak at 600 K can therefore only be clearly identified up to an iron content of 3.3% (w/w) before it becomes a shoulder of the peak at 680–700 K for Z23 containing more iron. These samples also show intensified hydrogen consumption at temperatures higher than 750 K in which the peaks become more separated. With increasing iron content peaks with maxima at 820 and 970 K seem to be slightly shifted to higher temperatures. The samples with the highest iron contents, Z23Fe3.88 and Z23Fe4.22, reveal also an additional peak at 1150 K, near the maximum TPR temperature, so that the whole TPR profile of these samples becomes very similar to that of SM27Fe4.98 [34]. The total hydrogen consumption per mole iron decreased with rising iron contents from 0.86 to 1.30 (Table 1). This supports that a complete reduction to Fe(0) cannot be achieved when Z23 contains higher iron amounts. After deconvoluting the TPR profiles, the ratio between H_2 consumption at high and low temperatures increased from 3 to 5 for samples containing up 3.3% (w/w) Fe, but was >10 for samples containing more iron (limit temperature = 740 K). This finding and the increasing number of peaks support that Z23 with at least 3.3% (w/w) Fe contains numerous iron species, including also crystalline Fe_2O_3, which corresponds to the aforementioned characterisation results.

TPR profiles of Z50 were similar to those of Z23, but shifted to lower temperatures (start of reduction at ≈450 K) (Fig. 7(B)). Z50Fe0.93 exhibits peaks with maxima at 540 K, 600 K and 730 K. In addition, a broad shoulder in the range of 850 and 1173 K is also visible, in contrast to Z23Fe0.86. Although the total H_2/Fe ratio was comparable, the ratio between high and low temperature H_2 consumption was higher than that of Z23Fe0.86. Higher iron contents in Z50 do not alter position and area of peaks at temperatures < 660 K as compared to Z50Fe0.93, but at higher temperatures H_2 consumption significantly increases, resulting in a broad peak with a maximum at 900 K unfinished until the maximum TPR temperature. The total H_2/Fe ratio for Z50Fe2.65 decreased to 1.0, but ratio between high and low temperature H_2 consumption, >10, was higher (limit temperature = 740 K). This indicates that Z50Fe2.65 contains mostly multinuclear oxide clusters.

The TPR profiles of the Z280 samples were found to be different to those of Z23 and Z50. Hydrogen consumption started at the highest temperature (≈540 K) and shows one maximum at 820 K for Z280Fe1.13. Hydrogen consumption for Z280Fe3.60 shifted to 870 K and exhibited an additional peaks at temperatures higher than 1000 K. Both of the Z280 samples revealed no low-temperature H_2 consumption.

In the conclusion, it can be assumed that Z23 and Z50 contain charge compensating cations and well dispersed nanosized iron oxide clusters whilst Z280 contains only the latter. Since Si/Al ratio of the zeolite and/or the density of negative charges affected the position of the reduction peaks, some reference samples were investigated to relate certain peaks with known iron species.

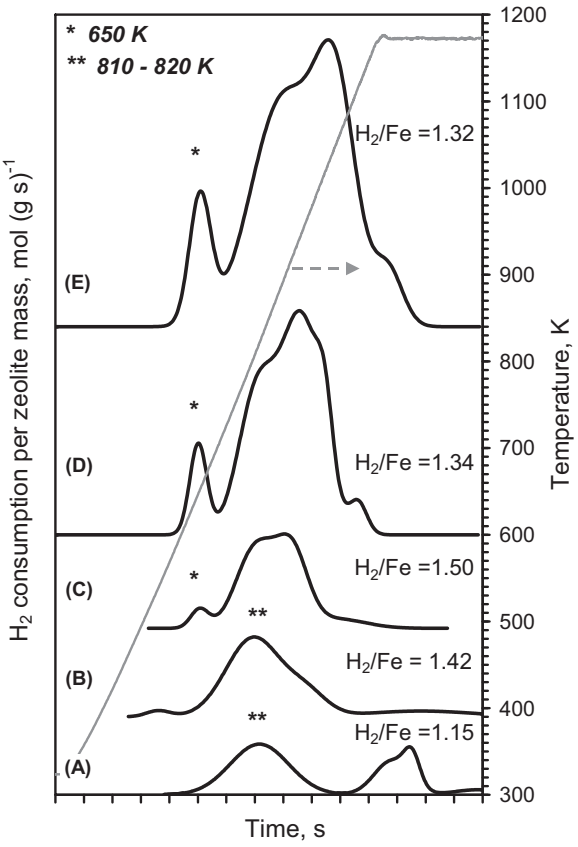

Fig. 8. TPR with H_2 of reference samples: (A) silica impregnated with Fe(III)nitrate (1.0% Fe (w/w)), physical mixtures: (B) Fe_2O_3/silica – 996 ppm Fe (w/w), (C) Fe_2O_3/Na-MFI – 992 ppm Fe (w/w), (D) Fe_2O_3/Na-MFI – 3.225% Fe (w/w), (E) Fe_2O_3/Na-MFI – 5.0% Fe (w/w).

Firstly, several physical mixtures of α-Fe_2O_3 with a zeolite in Na-form (Si/Al = 11.5) were used (Fig. 8) in which an ion exchange can be excluded [54]. Iron contents were chosen to cover the range of iron in solid-state exchanged zeolites. All mixtures show a sharp peak at 650 K which is higher than the temperature of first peaks in TPRs of Z23 and Z50, but lower than those observed for the Z280 samples (Fig. 7). The second peak of the mixtures is very broad at temperatures higher than 720 K. The total H_2/Fe ratio decreased from 1.5 to 1.32 with increasing iron content, showing that also Fe(III) in crystalline Fe_2O_3 cannot completely be reduced to Fe(0) up to 1173 K for higher iron contents. Nevertheless, H_2/Fe ratios are significantly higher than those found for corresponding solid-state exchanged Z23 and Z50 samples. In all physical mixtures, the H_2/Fe ratio of 0.15–0.17 regarding only the first peak and the ratio between high and low temperature hydrogen consumption of about 8–9 support the reduction sequence $Fe_2O_3 \rightarrow Fe_3O_4 \rightarrow Fe(0)$ [24,33–35,48,52]. These high ratios were only found for zeolites with high iron contents, for Z23Fe3.88 and Z50Fe2.65. However, TPR profiles of physical mixtures are still different from solid-state exchanged zeolites.

TPR profiles obtained for Z280 can be compared to TPRs of iron containing SiO_2 (Fig. 8) because of comparably low density of acid sites. The physical mixture α-Fe_2O_3/silica and silica impregnated with $Fe(NO_3)_3$ (1% (w/w) Fe) show a broad peak with a maximum at 810–820 K matching the temperature of the peak for Z280Fe1.13. However, only the H_2/Fe ratio of the impregnated silica corresponds to that of Z280Fe1.13 and the physical mixture consumes almost as much H_2 as necessary for the complete reduction down to Fe(0). Reduction of Fe(III) oxospecies supported on silica are assumed to proceed only to Fe(II) because of their interaction with silanol groups [55,56]. A further reduction to Fe(0) of these species starts at temperatures of 1100 K [31] as also indicated for the present impregnated silica and commonly assumed for the reduction of Fe(II) to Fe(0) in cationic species. Thus, the similarities between Z280Fe1.13 and impregnated silica indicate that latter one contains well-dispersed nanosized iron-oxo-clusters mainly interacting with silanol groups due to the low density of Brønsted acid sites. Moreover, TPRs of impregnated silica support that H_2 consumption peaks at temperatures higher than 700 K for Z23 and Z50 with less than 3.3% Fe (w/w) (Fig. 7) stand for the reduction of nanosized iron-oxo-species inside the channels of these zeolite (Table 1).

The low H_2/Fe ratios of most of the zeolites can result from the presence of iron cations and nanosized clusters irreducible up to the maximum TPR temperature. However, such low ratios may also result from iron(II) species which are either initially present in the zeolites or formed during the pretreatment in helium at 773 K due to autoreduction as reported by other groups [20,24,29,33,41]. In order to prove if this affects so far made conclusions, several samples were calcined in molecular oxygen at 823 K for 2 h before TPR (Fig. 7, thin lines). Since a H_2/Fe ratio of 1.5 was still not achieved (Table 1, numbers in brackets), it supports that iron forms in deed iron cations and well dispersed nanosized oxo clusters irreducible down to Fe(0) in the zeolites. However, even lower H_2/Fe was determined than after the pre-treatment in helium for samples containing less than 3% Fe (w/w) in contrast to findings of Lobree et al. [33]. Moreover, TPR profiles were changed after the pre-treatment in O_2. Peaks and shoulders at temperatures <650 K and >1000 K, particularly for Z23 and Z50 zeolites, were significantly reduced or disappeared whilst H_2 consumption increased in between these temperatures. The dependency of TPR profiles on the pre-treatment atmosphere displays a transformation of iron species that is usually not realised from TPR investigations because iron containing zeolites are commonly treated in O_2 before TPR to oxidise all iron to Fe(III). It has further to be mentioned that the pre-treatment atmosphere did not affect the profiles, peaks' position and H_2/Fe ratio for the physical Fe_2O_3/Na-MFI-mixtures and iron containing silica. Thus, this transformation belongs mainly to cations and well dispersed iron-oxo-species inside the zeolite channels, but cannot fully be explained at the moment. Nevertheless, this transformation can be responsible for a diminished surface oxygen formation in zeolites pre-treated in air.

4. Conclusions

The formation and stability of surface oxygen were investigated on ZSM-5 zeolites with different elemental composition using a transient multipulse technique combined with subsequent TPD. Various iron amounts were introduced into the NH_4— form of zeolites with different Si/Al ratio through a solid-state exchange with $FeCl_2$. Although more characterisation methods have to be applied in order to derive a clearer and quantitative picture about the iron species in our zeolites, the following conclusions can be made:

- Higher iron contents lead to an enhanced formation of surface oxygen, but only up to a certain extent, because bulky iron oxide clusters and crystalline Fe_2O_3 formed at Fe/Al > 0.5 does not significantly contribute to surface oxygen formation. The latter however contribute the sorption of molecular N_2O.
- The Si/Al ratio of the parent zeolite indirectly affects the surface oxygen formation because it represents the density of negative charges in the zeolite influencing the formation of certain iron species. However, it seems to exist an optimal Si/Al ratio for providing an appropriate mixture of well dispersed iron species which maximizes surface oxygen formation. These well dispersed

species are assumed to be cations, but mainly nanosized multinuclear oxide clusters. The impact of the latter on surface oxygen formation can be observed if iron is introduced in ZSM-5 zeolites with a high Si/Al ratio of ≈120.

- Autoreduction in helium at 773 K enhances the surface oxygen formation whilst treatment in O_2 blocks responsible sites. It can be assumed so far that Fe(II) ions in well dispersed nanosized oxide clusters which are formed directly in the solid-state exchange or during autoreduction, are oxidised by O_2. This transformation of iron species also leads to a less facile desorption of surface oxygen deposited in the N_2O activation.
- Higher iron contents lead to a more facile desorption of surface oxygen species, but it is also indicated that different surface oxygen species are present which may be initially bound to different sites. Zeolites containing bulky iron oxide clusters also release additional oxygen present as anion in the oxides. Nanosized iron oxide clusters present in zeolites with high Si/Al ratio form thermally most stable surface oxygen species.
- Results obtained in the multipulse experiments combined with TPD at atmospheric pressure were different to those obtained in the closed vacuum set-up of Panov and co-workers. These differences implying amount of formed surface oxygen and its desorption behaviour are most likely due to different operating conditions which results in a different status of the zeolite before and during the measurements, namely the degree of dehydroxylation and presence of gaseous and adsorbed impurities. Therefore, any findings concerning surface oxygen formed at atmospheric pressure can hardly be consistent with the definition for α-oxygen given by Panov et al.

Acknowledgements

Ayten Ates would like to thank DAAD – International Seminars, The Scientific & TUBITAK (Türkey) – DFG (Germany) for financial supports. The authors are very grateful to Prof. Dr. G.I. Panov, Dr. E. Starokon for providing the possibility to determine the α-oxygen content of several samples and to Dr. L. Pirutko for doing the elemental analysis of all samples.

References

[1] G.I. Panov, A.K. Uriarte, M.A. Rodkin, V.I. Sobolev, Catal. Today 41 (1998) 365–385.
[2] G. Centi, G. Giordano, P. Fejes, A. Katovic, K. Lazar, J.B. Nagy, S. Perathoner, Stud. Surf. Sci. Catal. 154 (2004) 2566–2573.
[3] K. Nowinska, A. Waclaw, A. Izbinska, Appl. Catal. A 243 (2003) 225–236.
[4] E.V. Kondratenko, J. Perez-Ramirez, Appl. Catal. A 267 (2004) 181–189.
[5] V. Duma, D. Hönicke, J. Catal. 191 (2000) 93–104.
[6] Q. Zhang, Q. Guo, X. Wang, T. Shishido, Y. Wang, J. Catal. 239 (2006) 105–116.
[7] G.I. Panov, K.A. Dubkov, E.V. Starkon, Catal. Today 117 (2006) 148–155.
[8] K.A. Dubkov, N.S. Ovanesyan, A.A. Shteinman, E.V. Starokon, G.I. Panov, J. Catal. 207 (2002) 341–352.
[9] Q. Zhu, R.M. van Teeffelen, R.A. van Santen, E.J.M. Hensen, J. Catal. 221 (2004) 575–583.
[10] G.D. Pringruber, P.K. Roy, Catal. Today 110 (2005) 199–210.
[11] T. Nobukawa, M. Yoshida, S. Kameoka, S.I. Ito, K. Tomishige, K. Kunimori, Catal. Today 93 (2004) 791–796.
[12] T. Nobukawa, K. Sugawara, K. Okumura, K. Tomishige, K. Kunimori, Appl. Catal. B 70 (2007) 342–352.
[13] S. Kameoka, T. Nobukawa, S. Tanaka, S. Ito, K. Tomishige, K. Kunimori, Phys. Chem. Chem. Phys. 5 (2003) 3328–3333.
[14] E.J.M. Hensen, Q. Zhu, M.M.R.M. Hendrix, A.R. Overweg, P.J. Kooyman, M.V. Sychev, R.A. van Santen, J. Catal. 221 (2004) 560–574.
[15] P. Marturano, L. Drozdova, A. Kogelbauer, R. Prins, J. Catal. 192 (2000) 236–247.
[16] El.-M. El-Malki, R.A. van Santen, W.M.H. Sachtler, J. Catal. 196 (2000) 212–223.
[17] B.J. Wood, J.A. Reimer, A.T. Bell, M.T. Janicke, K.C. Ott, J. Catal. 224 (2004) 148–155.
[18] L. Kiwi-Minsker, D.A. Bulushev, A. Renken, J. Catal. 219 (2003) 273–285.
[19] J. Perez-Ramirez, M.S. Kumar, A. Brückner, J. Catal. 223 (2004) 13–27.
[20] E. Berrier, O. Ovsitser, E.V. Kondratenko, M. Schwidder, W. Grünert, A. Brückner, J. Catal. 249 (2007) 67–78.
[21] K. Sugawara, T. Nobukawa, M. Yoshida, Y. Sato, K. Okumura, K. Tomishige, K. Kunimori, Appl. Catal. B 69 (2007) 154–163.
[22] A. Guzman-Vargas, G. Delahay, B. Coq, Appl. Catal. B 42 (2003) 369–379.
[23] K. Krishna, M. Makkee, Catal. Lett. 106 (2006) 183–193.
[24] R. Joyner, M. Stockenhuber, J. Phys. Chem. B 103 (1999) 5963–5976.
[25] M.S. Kumar, M. Schwidder, W. Grünert, A. Brückner, J. Catal. 227 (2004) 384–397.
[26] H.Y. Chen, W. Sachtler, Catal. Today 42 (1998) 73–83.
[27] El-M. El-Malki, R. van Santen, W. Sachtler, J. Phys. Chem. B 103 (1999) 4611–4622.
[28] A.A. Battiston, J.H. Bitter, F.M.F. de Groot, A.R. Overweg, O. Stephan, J.A. van Bokhoven, P.J. Kooyman, C. van der Spek, G. Vanko, D.C. Koningsberger, J. Catal. 213 (2003) 251–271.
[29] G.D. Pirngruber, P.K. Roy, R. Prins, J. Catal. 246 (2007) 147–157.
[30] G.D. Pirngruber, P.K. Roy, R. Prins, Phys. Chem. Chem. Phys. 8 (2006) 3939–3950.
[31] K. Sun, H. Xia, E. Hensen, R. van Santen, C. Li, J. Catal. 238 (2006) 186–195.
[32] M. Kögel, R. Mönnig, W. Schwieger, A. Tissler, T. Turek, J. Catal. 182 (1999) 470–478.
[33] L.J. Lobree, I.C. Hwang, J.A. Reimer, A.T. Bell, J. Catal. 186 (1999) 242–253.
[34] A. Ates, A. Reitzmann, J. Catal. 235 (2005) 164–174.
[35] F. Heinrich, C. Schmidt, E. Löffler, M. Menzel, W. Grünert, J. Catal. 212 (2002) 157–172.
[36] B.M. Abu-Zeid, W. Schwieger, A. Unger, Appl. Catal. B 84 (2008) 277–288.
[37] G.D. Pirngruber, M. Luechinger, P.K. Roy, A. Cecchetto, P. Smirniotis, J. Catal. 224 (2004) 429–440.
[38] E.V. Starokon, K.A. Dubkov, L.V. Pirutko, G.I. Panov, Top. Catal. 23 (2003) 137–143.
[39] A. Ates, A. Reitzmann, Chem. Eng. J. 134 (2007) 218–227.
[40] J. Perez-Ramirez, E.V. Kondratenko, M.N. Debbagh, J. Catal. 233 (2005) 442–452.
[41] J. Jia, K.S. Pillai, W.M.H. Sachtler, J. Catal. 221 (2004) 119–126.
[42] Q. Zhu, B.L. Mojet, R.A.J. Jaonssen, E.J.M. Hensen, J. Van Grondella, P.C.M.M. Magusin, R.A. Van Santan, Catal. Lett. 81 (2002) 205–212.
[43] A. Heyden, A.T. Bell, J.F. Keil, J. Catal. 233 (2005) 26–35.
[44] D.A. Bulushev, P.M. Prechtl, A. Renken, L. Kiwi-Minsker, Ind. Eng. Chem. Res. 46 (2007) 4178–4185.
[45] G.I. Panov, E.V. Starokon, L.V. Pirutko, E.A. Paukshtis, V.N. Parmon, J. Catal. 254 (2008) 110–120.
[46] D.A.M. Monti, A. Baiker, J. Catal. 83 (1983) 323–335.
[47] S. Bordiga, R. Buzzoni, F. Geobaldo, C. Lamberti, E. Giamello, A. Zecchina, G. Leofanti, G. Petrini, G. Tozzola, G. Vlaic, J. Catal. 158 (1996) 486–501.
[48] M. Yoshida, T. Nobukawa, S.I. Ito, K. Tomishige, K. Kunimori, J. Catal. 223 (2004) 454–464.
[49] T. Nobukawa, M. Yoshida, K. Okumura, K. Tomishige, K. Kunimori, J. Catal. 229 (2005) 374–388.
[50] C.S. Triantafillidis, A.G. Vlessidis, L. Nalbandian, N.P. Evmiridis, Microporous Mesoporous Mater. 47 (2001) 369–388.
[51] G. Delahay, D. Valade, A. Guzman-Vargas, B. Coq, Appl. Catal. B 55 (2005) 149–155.
[52] I. Melian-Cabrera, S. Espinosa, J.C. Groen, B. Linden, F. Kapteijn, J.A. Moulijn, J. Catal. 238 (2006) 250–259.
[53] P.K. Topsфe, E.G. Derouane, J. Catal. 70 (1981) 41–52.
[54] M.S. Batista, M. Wallau, E.A. Urquieta-Gonzales, Braz. J. Chem. Eng. 22 (2005) 341–351.
[55] F. Arena, G. Gatti, G. Martra, S. Coluccia, L. Stievano, L. Spadaro, P. Famulari, A. Parmaliana, J. Catal. 231 (2005) 365–380.
[56] P. Decyk, M. Trejda, M. Ziolek, J. Kujawa, K. Głaszczka, M. Bettahar, S. Monteverdi, M. Mercy, J. Catal. 219 (2003) 146–155.